Kinetic Parameters for Step and Flash Imprint Lithography Photopolymerization

Michael D. Dickey and C. Grant Willson
Dept. of Chemical Engineering, The University of Texas, Austin, TX 78712

DOI 10.1002/aic.10666
Published online October 26, 2005 in Wiley InterScience (www.interscience.wiley.com).

Step and Flash Imprint Lithography (SFIL) is a high-resolution, yet low-cost nanopatterning technique that employs an acrylate-based, free-radical photo-polymerization to replicate a patterned template onto a substrate. Modeling the photo-polymerization requires knowledge of the values of several reaction parameters, which are unique to the acrylate formulation used in SFIL. The values of these parameters were experimentally determined for use in a previously described kinetic model. The rate coefficient for initiation, k_i, was determined by measuring the absorbance spectrum of the initiator, Darocur® 1173, and convolving it with the intensity spectrum from the irradiation source. The reaction coefficients k_p and k_t were measured using the dark polymerization method. The experimental values of both parameters were then mathematically modeled to reflect the changes that occur as a function of conversion. Measuring the kinetic parameters provides insight into the fundamental steps involved in the polymerization. © 2005 American Institute of Chemical Engineers *AIChE J,* 52: 777–784, 2006
Keywords: nanoimprint lithography, reaction kinetics, photopolymerization, free-radical rate coefficients

Introduction

Photolithography is a technology that has enabled the microelectronics industry to print ever-smaller electronic components. Step and Flash Imprint Lithography (SFIL), as shown in Figure 1, offers a high resolution, low cost alternative to conventional lithographic printing techniques.[1-3] The recent inclusion of imprint lithography in the International Technology Semiconductor Roadmap is indicative of the heightened interest in imprinting technology.[4]

One of the distinguishing aspects of SFIL is the use of a photo-curable acrylate-based etch barrier. During the exposure step, as seen in Figure 1, the etch barrier is photo-cured via a free-radical polymerization. Understanding the kinetics of the photocuring step is critical for the optimization of SFIL processing. The photocuring step impacts the imprinting throughput and the mechanical properties of the resulting polymer. Photocuring is significantly affected by oxygen, a well known free-radical inhibitor.[5] At the beginning of the polymerization, atmospheric oxygen dissolved in the etch barrier causes an inhibition period. Polymerization only proceeds once the dissolved oxygen is sufficiently consumed to allow the monomer to compete successfully with the oxygen for initiating radicals,[5] which ultimately lowers the throughput of SFIL. During the polymerization, oxygen diffuses into the etch barrier from the perimeter of the template, as seen in Figure 2a. This results in a ring of undercured, tacky material surrounding the perimeter of the etch barrier, as seen in Figure 2b. This under-cured material may stick to the template, which could foul the template and contribute to defect generation during subsequent imprints. Recently, a model was described that can be used to quantify the inhibitory effects of oxygen on the SFIL process.[6] The model requires measurement of the kinetic parameters in the SFIL process, which is the focus of this article.

Materials and Procedure

The composition of the current SFIL etch barrier is given in Table I. The details surrounding this formulation are given elsewhere.[6]

Real time – Fourier transform infrared (RTIR) spectroscopy

Correspondence concerning this article should be addressed to C. G. Willson at willson@che.utexas.edu.

© 2005 American Institute of Chemical Engineers

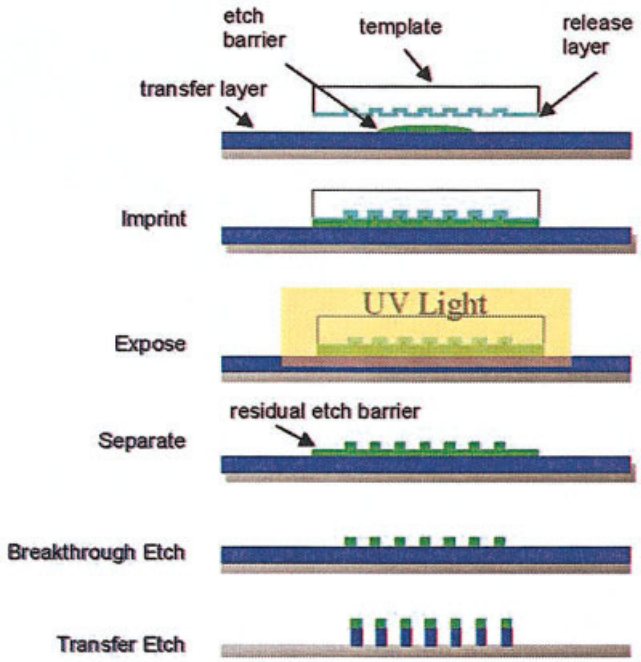

Figure 1. The SFIL process.

A photocurable acrylate-based material is dispensed onto a substrate. The material is pressed into a molded template and irradiated through the template by UV light. The template is removed, leaving behind a replica of the mold. A series of selective etch steps results in high aspect ratio patterned features. [Color figure can be viewed in the online issue, which is available at www.interscience.wiley.com.]

was used to monitor the etch barrier polymerization. RTIR utilizes *in situ* IR measurements to track the disappearance of acrylate double bonds during photocuring. A Nicolet Magna-IR 550 was used at 8 cm^{-1} resolution, which allowed for measurements every 0.07 s. Samples were prepared by placing a drop of etch barrier solution on a double polished silicon wafer. The drop was covered with a sodium chloride disk (Wilmad). The salt disk forced the drop to form a thin film and provided a barrier to prevent oxygen diffusion during curing. Dissolved oxygen was not removed from the etch barrier.

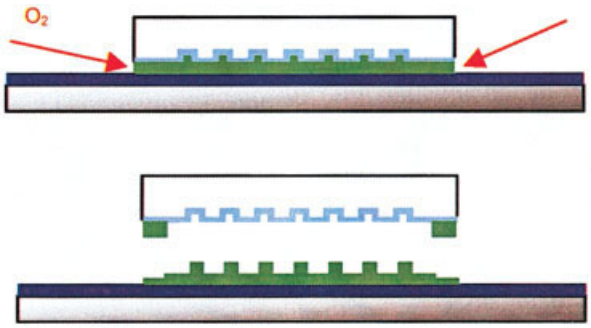

Figure 2. (a) Oxygen diffuses into the perimeter of the etch barrier under the template, and (b) Undercured material remains on template, potentially affecting subsequent imprints.

[Color figure can be viewed in the online issue, which is available at www.interscience.wiley.com.]

Table 1. Etch Barrier Composition

Component	Purpose	Weight Percent
Gelest SIA-0210 (SIA)	Silicon Containing Monoacrylate for Etch Resistance	44
Ethylene Glycol Diacrylate (EGDA)	Cross-linker	15
t-Butyl Acrylate (TBA)	Reactive diluent	37
Darocur 1173	Photoinitiator	1–4

Monomers were used as received: TBA (98%, Aldrich 327182), EGDA (96%, Aldrich 480797), and SIA (Gelest SIA0210.0). Typically, commercial acrylates contain a small level (10–20 ppm) of MEHQ (Hydroquinone monomethyl ether) inhibitor to provide stability during shipping. The inhibitor was not removed since the low levels of MEHQ in the monomers do not have a significant impact on the kinetics. The polymerizations were irradiated with a mercury lamp (Novacure EFOS) at 31.8 mW/cm^2 to mimic the lamp in our SFIL tool,[7] unless otherwise noted. The polymerizations were all performed under normal, ambient atmospheric conditions.

Theory: SFIL Kinetic Model

A model for the SFIL kinetics described in a previous article[6] is based on classical free-radical polymerization kinetics.[8] The equations from that model are summarized for the benefit of the reader

$$\text{Initiator: } \frac{d[I]}{dt} = -\Phi' k_I [I] \tag{1}$$

$$\text{Radicals: } \frac{d[R]}{dt} = 2\Phi k_I[I] - k_{O2}[O_2][R] - 2k_t[R]^2 \tag{2}$$

$$\text{Oxygen: } \frac{d[O_2]}{dt} = D_{O_2} \frac{\partial^2 [O_2]}{\partial x^2} - k_{O2}[O_2][R] \tag{3}$$

$$\text{Monomer: } \frac{d[M]}{dt} = -k_p[M][R] \tag{4}$$

Equations 1–4 account for the concentration of the four components in the system, initiator (I), radicals (R), oxygen (O_2), and monomer (M). The brackets ([. . .]) in Eqs. 1–4 are indicative of concentration (mol/L). Equation 3 includes a term that accounts for oxygen diffusion, based on Fick's second law, which requires knowledge of the diffusion coefficient for oxygen, D (cm^2/s) in the SFIL etch barrier.

The computer-based simulation of this model is summarized elsewhere with the appropriate boundary conditions. The measurement of the diffusion coefficient of oxygen and the oxygen reaction coefficient, $k_{02,}$ are also discussed elsewhere.[6]

The focus of this work is on determining the kinetic parameters. The reaction coefficient for initiation k_I, represents the amount of light absorbed per mole of initiator. We define the quantum yield of initiation Φ, as the product of two terms, $\Phi = \Phi' f$, where f is the initiator efficiency (fraction of radicals

produced that initiate propagating chains), and Φ', the number of initiator molecules dissociated per photon absorbed.[5,9] The coefficient of polymerization k_p, and the rate coefficient of termination k_t, are two critical rate coefficients for the model. Note that these coefficients are not rate "constants" because they are highly dependent on conversion.[10] Consequently, effects such as autoacceleration and autodeceleration can be accounted for by measuring these coefficients as functions of conversion. These effects are explained thoroughly elsewhere.[10,11]

Methodology: Determining Rate Coefficients

Determining the explicit values of the individual rate coefficients k_p and k_t is not a trivial task.[12] In fact, an IUPAC committee has been working for the past 15 years to address the most appropriate way to measure rate coefficients.[10] The committee recommends using a combination of the pulsed-laser polymerization (PLP) method to find k_p, and a single pulse-pulsed laser polymerization (SP-PLP) to find k_t.[10] PLP typically determines k_p only at low conversions, and then extends those values over all conversions since propagation is chemically controlled.[13,14] The PLP method has proven to be very reliable, but unfortunately is not applicable to the etch barrier system due to the presence of crosslinker (EGDA), which prevents the use of size-exclusion chromotagraphy (SEC) necessary for the analysis.[15] In addition, the PLP method has proven to be difficult to apply to acrylates,[16,17] partly due to the skew in molecular-weight distribution caused by chain transfer.[18]

Initial attempts to measure the reaction coefficients involved using the "rotating sector" method. Unfortunately, this method proved to have several limitations, including its tedious nature. The rotating sector method has problems with unjustified assumptions, primarily due to the fact that the reaction environment is not necessarily constant from experiment to experiment.[10,17,19] An alternative kinetic analysis technique is electron spin resonance (ESR), which directly measures radical concentration, but it also has many challenges and difficulties associated with it.[12]

After evaluating several kinetic measurement techniques, the individual coefficients k_p and k_t were determined using an established two step procedure. The ratio $k_p/k_t^{0.5}$ can be obtained from the slope of a RTIR polymerization profile using a quasi-steady-state approximation, which was described elsewhere.[6] A second expression for k_p and k_t was then obtained using the dark polymerization method, which has literature precedence for both monofunctional [11,22-24] and multifunctional (that is, crosslinked) systems.[11,20-22,25-29] This nonsteady-state method involves halting the UV exposure at a certain point in the polymerization. The radicals that remain active after the light is turned off continue to contribute to polymerization until they are terminated. The resulting "dark" polymerization can be tracked by RTIR. The analysis of the resulting dark polymerization data gives a second expression for the reaction coefficients k_p/k_t. The individual coefficients k_p and k_t are calculated by combining the measured ratios k_p/k_t and $k_p/k_t^{0.5}$. The mathematical derivation for this method is explained by Decker.[22] Numerous runs were performed using this method, each time turning off the light source at a new point in the polymerization to allow for the measurement of the coefficients as a function of conversion. By taking measurements at various conversions, effects such as autoacceleration and autodeceleration can be accounted for in the model by establishing the relationship between k_p and k_t and conversion.[30] Fortunately, k_p and k_t do not change significantly during an individual dark polymerization measurement since the extent of conversion during a measurement is quite small (2–4%). The low extent of conversion during dark polymerization is due to the rapid rate of radical termination associated with acrylates. Radicals terminate most rapidly at low levels of overall conversion, where they have relatively high mobility. As a result, the contribution of RTIR noise to experimental error is largest when using the dark polymerization method at the beginning of the reaction, since the duration of the dark polymerization is relatively short.

The dark polymerization method requires assumption of the applicability of classical free-radical kinetics. The use of traditional kinetics is often justified by considering polymerization to consist of three main steps (initiation, polymerization, termination), where k_p and k_t are composite values that represent processes contributing to propagation and termination, which change with conversion to account for changes in reaction environment.[31] Previously,[6] it was shown that the etch barrier rate of polymerization is proportional to $(R_i/k_t)^{0.5}$, which is also a requisite of classical free-radical kinetics. R_i represents the rate of initiation, as defined in Eq. 5.

In order to perform the dark polymerization analysis, the rate of initiation must be known. Therefore, a portion of this work is dedicated to characterizing the initiation properties of the SFIL system.

Results: Determining Rate of Initiation

Understanding the rate of initiation, as shown below in Eq. 5, involves determining two terms, Φ and k_I. The reaction coefficient k_I depends solely on the amount of light absorbed by the initiator. Only a fraction of the absorbed photons result in propagating radical chains, as described by the quantum yield Φ.

k_I is derived in Eqs. 5–7 using a thin film approximation of Beer's Law. The thin film approximation is justified since the etch barrier thickness is only on the order of several hundred nanometers

$$\text{Rate of Initiation} = 2\Phi k_I[I] = 2\Phi I_{abs} \tag{5}$$

I_{abs} represents the moles of absorbed light per unit volume, which is defined by the thin film approximation of Beer's Law, as seen in Eq. 6. Equation 6 is a modified form of Beer's Law since both sides of the equation have been normalized by film thickness b. This approach makes the model insensitive to the thickness of the etch barrier

$$I_{abs} = I_0(2.3\varepsilon[I]) \tag{6}$$

I_0 is the incident light intensity upon the etch barrier film (mol of incident light/cm^2), and ε is the film's extinction coefficient (L/mol-cm). The factor of 2.3 derives from the conversion between log base 10 and natural log during linearization. Equations 5 and 6 can be combined to give k_I

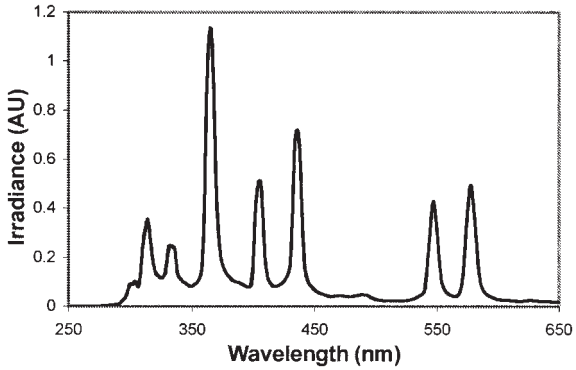

Figure 3. Relative intensity spectrum of Hg arc lamp used in prototype SFIL tool.

$$k_I = I_0(2.3\varepsilon) \tag{7}$$

Determining k_I is not trivial since both I_0 and ε are dependent on wavelength. Thus, the absorbance spectrum of Darocur 1173, and the light intensity spectrum for the exposure source must be convolved.[32] The lamp used in our prototype SFIL imprinting tool is a medium pressure mercury lamp, with the relative intensity spectrum shown in Figure 3. The extinction coefficient as a function of wavelength for Darocur 1173 initiator is shown in Figure 4.

The extinction coefficient was calculated after measuring the absorbance of a 0.054 wt % solution of Darocur 1173 in acetonitrile using UV–vis spectrometry. Since Darocur is highly absorbing below 300 nm, two different measurements were taken. A cuvette with a 0.1 cm path length was used to measure absorbance below 300 nm, and a cuvette cell with a path length of 1 cm was used to measure absorbance above 300 nm. The experimental values in Figure 4 agree with advertised values given by CIBA, the manufacturer of Darocur 1173.

Convolving the extinction coefficients from Figure 4, with the spectrum from Figure 3 gives the absorbed light intensity for Darocur 1173, I_{abs}. Normalizing this value to thickness and initiator concentration, which is justified by the Beer's Law thin film approximation, gives a k_I value of 6.7×10^{-3} (mol-photon/mol-I sec, where I represents initiator). It should be noted that this value is for a 32 mW/cm^2 exposure dose using a mercury lamp. However, this value scales linearly with intensity. The benefit of using the k_I format is that the value is independent of initiator concentration and film thickness as long as the thin film approximation holds. In addition, the k_I format is convenient for modeling the effects of varying light intensity and initiator absorbance on the polymerization with a single parameter k_I. The value of k_I does not change drastically with conversion, however efficiency does change.[10]

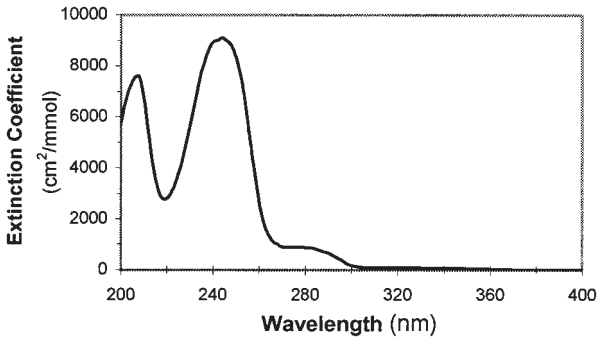

Figure 4. The extinction coefficient (cm^2/mmol) for Darocur 1173 as a function of wavelength.

The second parameter necessary for modeling the initiation process Φ, is generally very difficult to measure, and the few values that are reported in literature are system specific.[33] In fact, direct measurements of initiator efficiencies are nearly nonexistent.[34] There are several possible measurement methods, but none of these methods are applicable for the SFIL etch barrier (for example, end-group analysis, C^{13} NMR, deduction from emulsion studies using bulk data, RT-UV, and so on).[12,35] An unknown quantum yield is often addressed by putting data in terms of a relative radical concentration.[16] This has also been done by lumping efficiency with k_p.[25] Unfortunately, to effectively model the effects of oxygen on SFIL, the value of Φ must be known explicitly.

An estimation method was used to determine Φ for the SFIL etch barrier. The method requires measuring both the inhibition period at the beginning of the polymerization due to oxygen and the dissolved oxygen concentration. The inhibition period is due to the high reactivity of oxygen with free radicals ($k_{O2} \sim 10^9$ L/mol · s).[5,6] As radicals are generated by irradiation, they are immediately quenched in the presence of oxygen. Thus, an estimate of Φ can be determined by measuring the amount of time necessary to consume the oxygen (that is, the inhibition period). This method requires removing any inhibitor shipped with the monomers that would lengthen the inhibition period. This was done using a commercially available inhibitor remover (Aldrich 306312-1EA). Once purified and formulated, the etch barrier polymerization reaction was tracked using RTIR. The duration of the inhibition period was estimated as the time necessary to reach 1% conversion. If it is assumed that all active radicals are instantaneously consumed by oxygen, the initial concentration of oxygen divided by inhibition time gives the rate of initiation, as seen in Eq. 8. This of course assumes that the initiator concentration remains constant, which is a reasonable assumption for the rates of initiation used in this process (changes ~2% during the inhibition period).

$$\frac{d[O_2]}{dt} = 2\Phi k_I[I] = \frac{[O_2]_0}{Inhibition\ Time} \tag{8}$$

The initial concentration of oxygen was 2.8×10^{-4} mol/L at room-temperature, as measured using a dissolved oxygen probe (YSI-5100, YSI Environmental). The average inhibition time was 2.2 s for an incident intensity of 31.8 mW/cm^2, initiator concentration of 0.061 mol/L (~1 wt %), and k_I equal to 6.7×10^{-3} s^{-1}. Therefore, Φ is approximately 0.15 for the etch barrier formulation. Note that there was no significant difference in inhibition time for systems with removed inhibitor vs. those with inhibitor. This is consistent with literature results, which show that the induction period is overwhelmingly due to depletion of oxygen rather than MEHQ inhibitor (~500 ppm).[36] Thus, for the SFIL system there is no need to make an extra effort to remove inhibitor.

Although Φ is highly dependent on reaction environment, a

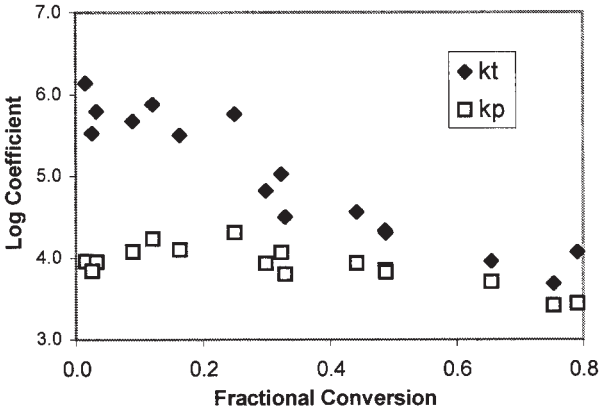

Figure 5. k_t and k_p (L/mol · s) measured for SFIL etch barrier (1 wt. % Darocur 1173, 31.8 mW/cm^2).

literature survey of Φ values in similar free-radical systems provides a valuable point of reference. The quantum yield of Darocur 1173 in benzene was reported to be 0.163 for 313 nm light.[37] Fouassier reports the quantum yield of Darocur 1173 to be 0.2 under practical conditions of bulk polymerization, based on time-resolved laser-spectroscopy.[38] Another study[39] reports a quantum yield of 0.25 for Darocur 1173, which is the value used in a study of butyl acrylates.[39,40] Irgacure 651 (dimethoxyphenylacetophenone, DMPA) is similarly structured to Darocur 1173. One study, using a fluorescence probe technique, showed that the quantum efficiency of Darocur 1173 is 0.73–0.88 times the quantum efficiency of Irgacure 651.[41] Thus, it may also be instructive to list several values of efficiency for Irgacure 651. Irgacure 651 has been shown to have quantum yields of 0.1, 0.4, 0.24, and 0.7 for various systems.[5,21,40,42,43] On the basis of these separate findings, our measured quantum yield (0.15) of Darocur 1173 in etch barrier is in the range of previously reported values.

It is well known that efficiency decreases with conversion.[44] As the network becomes more crosslinked and viscous, the cleaved radicals are more likely to recombine than diffuse apart to form new radical chains.[45] However, a study on butyl acrylate showed that k_p x Φ is constant well into the intermediate-conversion range, suggesting that Φ is independent of conversion over this range since k_p is known to be relatively constant.[12] For simplicity, we assume that the measured quantum efficiency of 0.15 is constant over the course of the polymerization. This assumption should only introduce significant error toward the final stages of conversion, where efficiency is known to drop rapidly. To compensate for this effect, the model allows the quantum efficiency to drop rapidly at high conversions to reflect the limited conversion observed experimentally (80–90% conversion).

Results: Determining k_p and k_t

Establishing the initiation properties for the etch barrier system allows for the measurement of the reaction coefficients k_t and k_p using the dark polymerization method. The resulting values of these coefficients as a function of conversion are displayed in Figure 5.

Figure 5 displays several trends typical of polymerization reactions. As expected, the value of k_p is relatively constant since the mobility of the monomer remains unhindered up to high levels of conversion (that is, polymerization is a chemically controlled process[13,46]). In contrast, k_t decreases by several orders of magnitude with increasing conversion due to the reduced mobility of macroradicals caused by changes in the reaction environment (that is, termination is a diffusion-controlled process [29]).

The initial plateau in k_t from 0 to 30% conversion is due to the high mobility of macroradicals at low conversion.[29] As the polymerization proceeds, and the reaction environment becomes more viscous, translational diffusion (diffusion of the center-of-mass of the polymer) begins to control the termination process, causing the k_t value to decrease dramatically, as seen between 30 and 40% conversion. The value of k_t is known to drop dramatically around the region where polymerization is most rapid.[29] After approximately 40% conversion, the value of k_t levels off, indicating a transition from translational diffusion to reaction diffusion.[18] The reaction diffusion concept was first introduced by Schulz, [47] and is explained thoroughly elsewhere.[25,26] Reaction diffusion occurs when the chain mobility is reduced to the point where termination primarily occurs by radical chains propagating toward each other via reaction with mobile monomer units. Since the termination reaction occurs via propagation, the respective rate coefficients become proportional. Thus, the reaction diffusion region is characterized by a plateau in the ratio k_t/k_p,[26] which appears to occur around 40% in the SFIL etch barrier system. As a basis for comparison, reaction diffusion has been observed at conversions as low as 5% in multifunctional systems, but typically occurs at ~50% conversion in linear systems.[26] Thus, the trends of Figure 5 are consistent for a system containing 15 wt % crosslinker. Furthermore, the k_t of typical crosslinked systems decreases drastically from 20–40% and then level out until about 80% conversion, at which point it is expected to decrease again.[10] Our data do not show a dramatic decrease at high conversion, but the error associated with determining rate coefficients at high conversion using the dark polymerization method is large when the slope (that is, rate of polymerization) is nearly zero.

Comparison of k_p and k_t with Previous Results

It might be misleading to compare the k_p and k_t values in Figure 5 with those in the literature, because the reported coefficients are overall rate coefficients specific to the SFIL etch barrier formulation. However, all of the components in the etch barrier are acrylates and k_p values of acrylates tend to show a family-type behavior.[46] Butyl acrylate is a commonly studied homopolymer reaction system. Although k_p is generally regarded as a chemically controlled process, it would be reasonable to expect the etch barrier k_p values to be slightly lower than a pure butyl acrylate system due to reduced mobility of the monomers in the etch barrier. In addition, the presence of the EGDA crosslinker causes the system to vitrify more rapidly than a monofunctional system. With that in mind, the PLP measurement method recommended by IUPAC found the k_p of butyl acrylate to be ~14,000 (L/mol · s) at 20 °C.[18] This is slightly higher than the k_p of the etch barrier, which hovers just below 10,000 (L/mol · s), as seen in Figure 5. The k_p for multiacrylates are typically on the order of 10,000 (L/mol · s), [29,48] which is consistent with the values in Figure 5.

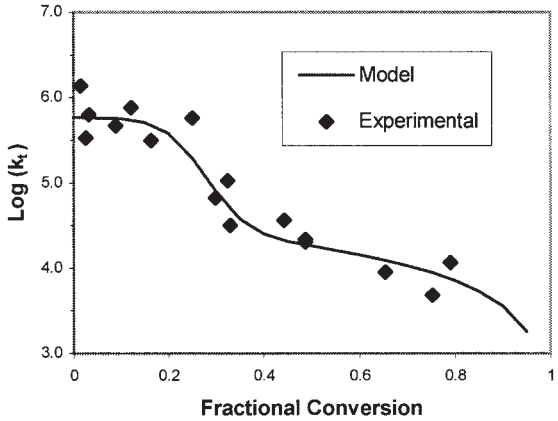

Figure 6. k_t data from Figure 5 fit with diffusion based model.

In contrast to k_p values, the k_t values in acrylates do not show a family-type behavior.[46] Termination is a diffusion controlled process, so it is reasonable to expect that the k_t value for the etch barrier will be between that of butyl acrylate, a highly mobile molecule, and that of a multifunctional, highly crosslinked system. The value of k_t for butyl acrylate is estimated to be between 10^7 and 10^8 (L/mol · s) at low conversions.[16] Typically, k_t is on the order of 10^7 (L/mol · s) for monoacrylate monomers at the beginning of reaction.[11] These values serve as a point of reference to understand the magnitude of k_t for small, monofunctional acrylates. As a point of contrast, k_t is reported to be on the order of 10^5 (L/mol · s) for multiacrylates.[48] Thus, it is expected that the etch barrier's k_t value should be between 10^5 (L/mol · s), which is the value for multiacrylates, and 10^7 (L/mol · s) for a highly mobile monofunctional acrylate. This is indeed the case at the beginning of the reaction, where k_t appears to be on the order of 10^6 (L/mol · s), but decreases rapidly with conversion due to gelation. This is clearly the case in the etch barrier polymerization, with k_t going from 10^6 at low conversions and decreasing to 10^4 (L/mol · s) after 40% conversion. Thus, it appears the results in Figure 5 are within the bounds of literature precedent.

Modeling k_p and k_t

A primary goal of the work described in this article was to develop an expression for k_p and k_t as a function of conversion for use in a previously developed kinetic model (Equations 1–4).[6] The value of k_p is not expected to vary significantly until high conversion (~80%) since it is a chemically controlled process,[14] however, little experimental evidence is available for high conversion k_p values.[18] The k_p values in the etch barrier are very consistent over the entire range of measured conversion, showing only a slight decrease at higher conversions. This trend is capturing using Eq. 9, where U is fractional conversion.[18] Equation 9 leads to a nearly constant value of k_p until high conversions. The constants k_{p0} and b were found to be 10.1 and 1.8, respectively, using a least-squares fit.

$$k_p = \frac{k_{p0}}{(1 + e^{bU})} \tag{9}$$

Table 2. Parameters for k_t Model

Parameter	Value	Units
$\ln(n_r)$	$28 \cdot U$	—
k_{TD}^0	2.6×10^8	L/mol · sec
$C_{RD} * k_p$	3.6×10^4	L/mol · sec
k_{SD}	5.5×10^5	L/mol · sec

Although k_p is relatively constant with conversion, k_t varies dramatically due to the extreme changes in reaction medium over the course of the polymerization.[10] The k_t data from Figure 5 can be fit with a model based on diffusion limited termination, as seen in Figure 6.[49] The model for k_t is based on a summation of the two dominant mechanisms that control termination, diffusion ($k_{t,D}$) and reaction diffusion ($k_{t,RD}$), as seen in Eq. 10. The relative value of these two terms as a function of conversion reflects the dominant termination mechanism. The maximum rate of polymerization can be thought of as the point where a shift occurs from $k_{t,D} \gg k_{t,RD}$ to $k_{t,RD} \gg k_{t,D}$.[29]

$$k_t = k_{t,D} + k_{t,RD} \tag{10}$$

The diffusion component is a combination of segmental diffusion (k_{SD}), which is a constant, and translational diffusion (k_{TD}), which is inversely proportional to relative viscosity (n_r) and directly proportional to translational diffusion at zero conversion (k_{TD}^0)

$$\frac{1}{k_{t,D}} = \frac{1}{k_{SD}} + \frac{1}{k_{TD}} \tag{11}$$

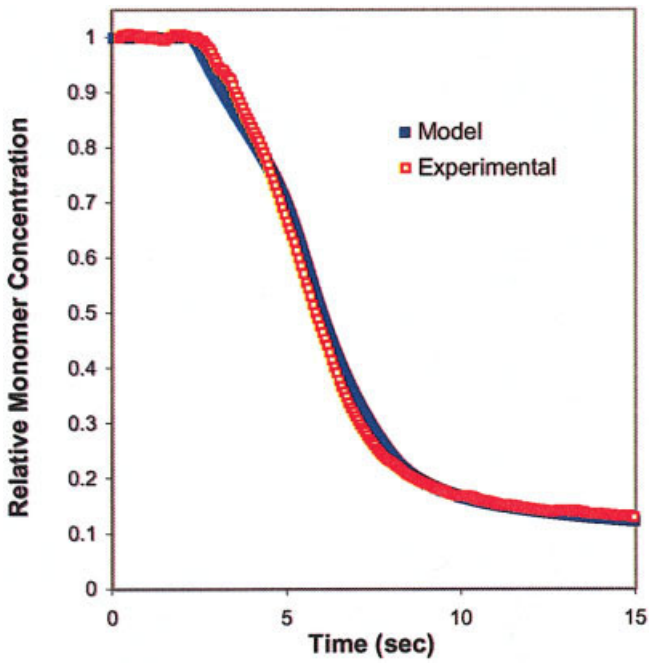

Figure 7. Experimentally determined kinetic data with model.

[Color figure can be viewed in the online issue, which is available at www.interscience.wiley.com.]

The reaction diffusion term is proportional to k_p, since reaction diffusion by definition involves propagating chain growth. C_{RD} is a reaction diffusion parameter and U is conversion

$$k_{t,RD} = C_{RD} \cdot k_p \cdot (1 - U) \tag{12}$$

The model in Eq. 10 was fit to the experimental data using a least-squares regression method. The parameters are shown in Table 2, and the resulting fit is shown in Figure 6. As seen in Figure 6, the model captures the trends of the data well.

Of course, the ultimate test of the validity of the experimental measurements, and the kinetic model is to incorporate the parameters into the model and compare the results with experimental observation. The result of this exercise is a fit in agreement with experimental data,[6] as shown in Figure 7. The only exception may be the very beginning of the polymerization (up to 20% conversion), where rate coefficients are difficult to measure due to the rapid rate of termination. A more detailed analysis of the SFIL etch barrier polymerization, which includes the incorporation of the kinetic parameters into a computer based model, is presented elsewhere. [6]

Conclusions

Values of the reaction parameters k_I, k_t, k_p, and Φ that are required to effectively model the effects of oxygen on the SFIL polymerization have been established. The rate coefficient for initiation k_I, was determined experimentally by measuring the absorbance of the initiator (Darocur 1173), and convolving it with the emission spectrum of the irradiation source. The quantum efficiency, Φ, was found to be 0.15 using an estimation method, based on the measurement of the initial oxygen inhibition period. The MEHQ inhibitor shipped with the commercial monomers makes no observable differences in the polymerization kinetics. The reaction coefficients k_p and k_t were measured using the dark polymerization method. The experimental values of both parameters were mathematically modeled to extract the changes in the values as a function of conversion, which helps account for effects, such as autoacceleration. The reaction parameters were shown to be consistent with literature precedent.

Acknowledgments

We thank Dr. Nick Stacey for valuable discussion and Dr. Todd Bailey for information on the SFIL exposure source. We thank the NSF for a graduate fellowship and DARPA Contract N66001-01-1-8964 for funding.

Literature Cited

1. Johnson SC, Bailey TC, Dickey MD, Smith BJ, Kim EK, Jamieson AT, Stacey NA, Ekerdt JG, Willson CG, Mancini DP, Dauksher WJ, Nordquist KJ, Resnick DJ. *Advances in Step and Flash Imprint Lithography.* Proceedings of SPIE-The International Society for Optical Engineering. 5037(Pt. 1, Emerging Lithographic Technologies VII): 2003;197-202.
2. Bailey TC, Johnson SC, Sreenivasan SV, Ekerdt JG, Willson CG, Resnick DJ. Step and flash imprint lithography: an efficient nanoscale printing technology. *J of Photopolymer Sci and Technol*. 2002;15(3): 481-486.
3. Bailey T, Smith B, Choi BJ, Colburn M, Meissl M, Sreenivasan SV, Ekerdt JG, Willson CG. Step and flash imprint lithography: Defect analysis. *J of Vacuum Sci & Technol, B: Microelectronics and Nanometer Structures*. 2001;19(6):2806-2810.
4. *International Technology Roadmap for Semiconductors*. Semiconductor Industry Association: San Jose, CA; 2003.
5. Decker C, Jenkins AD. Kinetic approach of oxygen inhibition in ultraviolet- and laser-induced polymerizations. *Macromolecules*. 1985;18(6):1241-4.
6. Dickey MD, Burns RL, Kim EK, Johnson SC, Stacey NA, Willson CG. A study of the kinetics of step and flash imprint lithography photopolymerization. *AIChE J*. 51(9):2547–2555.
7. Choi BJ. Johnson SC, Sreenivasan SV, Colburn M, Bailey TC, Willson CG. Partially Constrained Compliant Stages for High Resolution Imprint Lithography. in *Proc. ASME DETC2000*; 2000.
8. Odian GG. *Principles of Polymerization*. 3rd ed. New York: Wiley; 1991;22:768.
9. Kurdikar DL. Peppas NA. Kinetics of photopolymerizations of multifunctional monomers. *Polymeric Mat Sci and Eng*. 1993;69:174-5.
10. Buback M. Egorov M, Gilbert RG, Kaminsky V, Olaj OF, Russell GT, Vana P,. Zifferer G. Critically evaluated termination rate coefficients for free-radical polymerization, 1: The current situation. *Macromolecular Chem and Phys*. 2002;203(18):2570-2582.
11. Decker C, Elzaouk B, Decker D. Kinetic study of ultrafast photopolymerization reactions. *J of Macromolecular Sci, Pure and Appl Chem*. 1996;A33(2):173-90.
12. Buback M, Gilbert RG, Russell GT, Hill DJT, Moad G, O'Driscoll KF, Shen J, Winnik MA. Consistent values of rate parameters in free radical polymerization systems. II. Outstanding dilemmas and recommendations. *J of Poly Sci, Part A: Poly Chem* 1992;30(5):851-63.
13. Buback M. Initiation, propagation and termination in fluid phase free-radical polymerization. *Macromolecular Symposia 2001*. Polymerization Processes and Polymer Materials I: 2001;174:213-227.
14. Fischer JP, Schulz GV. Effect of solvent on the Arrhenius parameters of chain-growth and chain-breaking in the radical polymerization of methyl methacrylate. *Berichte der Bunsen-Gesellschaft*. 1970;74(10): 1077-82.
15. Lyons RA, Hutovic J, Piton MC, Christie DI, Clay PA, Manders BG, Kable SH,. Gilbert RG. Pulsed-laser polymerization measurements of the propagation rate coefficient for butyl acrylate. *Macromolecules*. 1996;29(6):1918-27.
16. Beuermann S. Paquet DA Jr, McMinn JH, Hutchinson RA. Determination of free-radical propagation rate coefficients of butyl, 2-ethylhexyl, and dodecyl acrylates by pulsed-laser polymerization. *Macromolecules*. 1996.29(12):4206-4215.
17. Van Herk AM. Pulsed initiation polymerization as a means of obtaining propagation rate coefficients in free-radical polymerizations. II Review up to 2000. *Macromolecular Theory and Simulations*. 2000; 9(8):433-441.
18. Beuermann S. Buback M. Rate coefficients of free-radical polymerization deduced from pulsed laser experiments. *Progress in Poly Sci*. 2002;27(2):191-254.
19. Hutchinson RA, Aronson MT, Richards JR. Analysis of pulsed-laser-generated molecular weight distributions for the determination of propagation rate coefficients. *Macromolecules*. 1993;26(24):6410-15.
20. Decker C, Elzaouk B. Photopolymerization of functional monomers. VII. Evaluation of the rate constants of propagation and termination. *EuroPoly J* 1995;31(12):1155-63.
21. Decker C, Moussa K. Kinetic investigation of photopolymerizations induced by laser beams. *Makromolekulare Chemie*. 1990;191(4): 963-79.
22. Decker C. The use of UV irradiation in polymerization. *Poly Intl*. 1998.45(2):133-141.
23. Williams RM. Khudyakov IV, Purvis MB, Overton BJ, Turro NJ. Direct and sensitized photolysis of phosphine oxide polymerization photoinitiators in the presence and absence of a model acrylate Monomer: A time resolved EPR, cure monitor, and photoDSC study. *J of Phys Chem B*. 2000;104(44):10437-10443.
24. Tryson GR, Shultz AR. A calorimetric study of acrylate photopolymerization. *J of Poly Sci, Poly Phys Ed*. 1979;17(12):2059-75.
25. Anseth KS. Wang CM, Bowman CN. Reaction behavior and kinetic constants for photopolymerizations of multi(meth)acrylate monomers. *Polymer*. 1994.35(15):3243-50.
26. Anseth KS, Wang CM, Bowman CN. Kinetic evidence of reaction diffusion during the polymerization of multi(meth)acrylate monomers. *Macromolecules*. 1994;27(3):650-5.
27. Anseth KS, Bowman CN, Peppas NA. Polymerization kinetics and volume relaxation behavior of photopolymerized multifunctional

monomers producing highly crosslinked networks. *J of Poly Sci. Part A: Poly Chem*.1994;32(1):139-47.
28. Decker C. Moussa K. Photopolymerization of polyfunctional monomers. III. Kinetic analysis by real-time IR spectroscopy. *Euro Poly J*. 1990;26(4):393-401.
29. Andrzejewska E. Photopolymerization kinetics of multifunctional monomers. *Progress in Poly Sci*. 2001;26(4):605-665.
30. Goodner MD. Bowman CN. Modeling primary radical termination and its effects on autoacceleration in photopolymerization kinetics. *Macromolecules*. 1999;32(20):6552-6559.
31. Khudyakov IV, MB, Purvis, Turro NJ. Kinetics of photopolymerization of acrylate coatings. *ACS Symposium Series 2003*. Photoinitiated Polymerization; 2003;847:113-126.
32. Mack CA.Absorption and exposure in positive photoresist. *Applied Optics*. 1988;27(23):4913-19.
33. Scherzer T, Decker U. Kinetic investigations on UV-induced photopolymerization reactions by real-time FTIR-ATR spectroscopy: The efficiency of photoinitiators at 313 and 222 nm. *Nuclear Instruments & Methods in Physics Research, Section B: Beam Interactions with Materials and Atoms*. 1999;151(1-4):306-312.
34. Buback M, Huckestein B, Kuchta F-D, Russell GT, Schmid E. Initiator efficiencies in 2,2'-azoisobutyronitrile-initiated free-radical polymerizations of styrene. *Macromolecular Chem and Phys*. 1994;195(6): 2117-40.
35. Buback M. Garcia-Rubio LH, Gilbert RG, Napper DH, Guillot J, Hamielec AE, Hill D, O'Driscoll KF, Olaj OF, and et al. Consistent values of rate parameters in free radical polymerization systems. *J of Poly Sci, Part C: Poly Lett.* 1988;26(7): 293-7.
36. Wight FR. Oxygen inhibition of acrylic photopolymerization. *J of Poly Sci, Poly Lett Ed*. 1978;16(3):121-7.
37. Lewis FD, Magyar JG. Photoreduction and.alpha. cleavage of aryl alkyl ketones. J. of Organic Chemistry. 1972;37(13):2102-7.
38. Fouassier JP. Polymerization photoinitiators: excited state processes and kinetic aspects. *Progress in Organic Coatings*, 1990;18(3):229-52.
39. Eichler J, Herz CP, Naito I, Schnabel W. Laser flash photolysis investigation of primary processes in the sensitized polymerization of vinyl monomers. IV. Experiments with hydroxy alkylphenones. *J of Photochem*. 1980;12(3):225-34.
40. BubackM, Degener B. Rate coefficients for free-radical polymerization of butyl acrylate to high conversion. *Makromolekulare Chemie*, 1993;194(10):2875-83.
41. Hu S, Popielarz R, Neckers DC. Fluorescence probe techniques (FPT) for measuring the relative efficiencies of free-radical photoinitiators. *Macromolecules*. 1998;31(13):4107-4113.
42. Mateo JL. Serrano J, Bosch P. Photopolymerization of Di- and tetrafunctional methacrylic monomers in a polymeric medium: Kinetics and evidence of reaction diffusion during an all photopolymerization reaction. *Macromolecules.* 1997;30(5):1285-1288.
43. Groenenboom CJ. Hageman HJ,Overeem T, Weber AJM. Photoinitiators and photoinitiation. 3. Comparison of the photodecompositions of.alpha.-methoxy- and.alpha.,.alpha.-dimethoxydeoxybenzoin in 1,1-diphenylethylene as model substrate. *Makromolekulare Chemie*.1982; 183(2):281-92.
44. Kurdikar DL, Peppas NA. Investigation of diffusion-controlled homopolymerization of bifunctional monomers. *Vysokomolekulyarnye Soedineniya, Seriya A i Seriya B*. 1994;36(11):1852-61.
45. Decker C. Real-time monitoring of polymerization quantum yields. *Macromolecules*. 1990;23(25):5217-20.
46. Buback M. Initiation and Termination Rates Associated with Free-Radical Polymerization in Extended Ranges of Temperature and Pressure. *ACS Symposium Series 2000*. Controlled/Living Radical Polymerization; 2000;768:39-56.
47. Schulz GV. Polymerization kinetics in highly concentrated systems. Kinetics of the Trommsdorf effect on methyl methacrylate. *Zeitschrift fuer Physikalische Chemie* (Muenchen, Germany). 1956;8:290-317.
48. Decker C. Kinetic study and new applications of UV radiation curing. *Macromolecular Rapid Communications*. 2002;23(18):1067-1093.
49. Buback M, Huckestein B, Russell GT. Modeling of termination in intermediate and high conversion free radical polymerizations. *Macromolecular Chem and Phys*.1994;195(2):539-54.

Manuscript received July 16, 2004, and revision received July 10, 2005.